View metadata, citation and similar papers at core.ac.uk
brought to you by CORE
provided by NASA Technical Reports Server

3 1176 00167 3582

NASA CR-164,181

JOINT INSTITUTE FOR AERONAUTICS AND ACOUSTICS

National Aeronautics and Space Administration
Ames Research Center

NASA-CR-164181
19810012780

Stanford University

JIAA TR - 33

ON THE PRESSURE FIELD OF NONLINEAR STANDING WATER WAVES

Leonard W. Schwartz

FOR REFERENCE
NOT TO BE TAKEN FROM THIS ROOM

STANFORD UNIVERSITY
Department of Aeronautics and Astronautics
Stanford, California 94305

MAY 1980

MAY 1 1981
LANGLEY RESEARCH CENTER
LIBRARY, NASA
Hampton, Virginia

NF01747

JIAA TR - 33

ON THE PRESSURE FIELD OF NONLINEAR STANDING WATER WAVES

LEONARD W. SCHWARTZ

MAY 1980

The work here presented has been supported by the
National Aeronautics and Space Administration under Contract
NASA NCC 2-55

N81-21309 #

ON THE PRESSURE FIELD OF
NONLINEAR STANDING WATER WAVES

Summary

The pressure field produced by two-dimensional nonlinear time-and space-periodic standing waves has been calculated as a series expansion in the wave height. The high-order series is summed by the use of Padé approximants. Calculations include the pressure variation at great depth, which is considered to be a likely cause of microseismic activity, and the pressure distribution on a vertical barrier or breakwater.

TABLE OF CONTENTS

Summary iii

Figure Captions v

1. Introduction 1

2. Mathematical Formulation and Results 4

References 12

Figures 13

Figure Captions

1. Time variation of pressure at infinite depth, $\varepsilon = 0.6$;

   - - - leading-order theory

2. Surface profiles versus time, $\varepsilon = 0.6$.

3. Magnitude of pressure variation at infinite depth;

   - - - leading-order theory

4. Pressure distribution vertically below a crest and a trough,

   $t = 0$, $\varepsilon = 0.55$.

1. Introduction

Standing waves characterize the sloshing ("seiching") of water in closed basins. They also arise, in effect, from the reflection of a wave train from a wall or coast and, in the open ocean, from the interaction of progressive wave trains.

For a two-dimensional progressive wave, the pressure field produced by the surface motion attenuates exponentially with depth. At depths of the order of a wavelength or greater, the difference between the progressive wave pressure field and the hydrostatic pressure is negligible. Plane time and space periodic standing waves arise from the interaction of two identical progressive wave trains moving in opposite directions. A remarkable feature of this interaction is the development of a time-varying component of pressure that acts upon the whole fluid simultaneously and is thus unattenuated with depth. In deep water, therefore, it is the dominant non-hydrostatic component. If ε is the dimensionless amplitude of the surface wave, this pressure component is of order ε^2. Because of the customary use of linear theory, this effect was long overlooked. It was apparently first recognized by Miche in 1944.

In a classical paper, Longuet-Higgins (1950) proposed a theory of the origin of microseisms based on this second-order pressure effect. He shows that the interference between groups of waves of the same frequency and travelling in opposite directions, arising from storms at sea, can produce ground movement of the observed frequency and order-

of-magnitude. It is remarkable that the frequency of this oscillatory pressure is twice that of the waves which produce it.

In a recent paper, Schwartz & Whitney (1980), hereafter referred to as SW , compute surface profiles and amplitude dispersion effects for nonlinear standing waves in deep water. The technique involves the calculation of these quantities as high-order series in the wave amplitude where the very substantial arithmetic manipulations are delegated to the computer. The calculations are greatly simplified by the introduction of a time-dependent conformal transformation that is used to map the moving fluid onto a fixed region in the tranformed plane. The series is computed to $O(\varepsilon^{25})$ and is summed by Padé approximants. The results are effectively exact except, perhaps, for waves within a few percent of the highest. A previous series computed by Penney and Price (1952), carried by hand to fifth-order, was found to be defective in the sense that their solution would force an unacceptable secular term at $O(\varepsilon^{6})$.

In this paper we use the series results from SW to compute the pressures on the sea bottom and a vertical breakwater produced by these standing waves. Because the unattenuated bottom effect is second-order in the amplitude and hence only significant for waves of moderate or greater steepness, a correct nonlinear solution is of particular importance here. It is shown that the simple leading-order theory used by Longuet-Higgins may overpredict the pressure variation for very steep waves by as much as 40 per cent. The variation of bottom pressure with time is also calculated for a steep wave; this pressure "signature" differs somewhat from a sinusoid. Finally we present the distribution

of pressures vertically below a crest and a trough at the instant of time when the surface displacement is a maximum. This may be interpreted as the variation of wave pressure upon a breakwater caused by normal incidence and reflection of a progressive wave train. The amplitude is chosen here so as to reproduce a similar calculation by Penney & Price. The present results differ from theirs in certain significant respects, however.

2. Mathematical Formulation and Results

The pressure p within an incompressible fluid moving irrotationally is given by the Bernoulli equation

$$\frac{p}{\rho} = -\phi_t - \frac{1}{2} w\bar{w} - gy \tag{1}$$

where ϕ is the velocity potential, w is the complex (conjugate) velocity $u - iv$, g the acceleration of gravity and ρ is the density. On the free surface the pressure is a constant which may, without loss of generality, be taken to be zero.

A "pure" standing wave that is periodic in both space and time is characterized by a frequency ω and a wave number k. Using $1/k$ and $1/\omega$ as units of length and time respectively, equation (1) may be written in dimensionless form as

$$\tilde{p} = -\frac{1}{S}\left(\tilde{\phi}_{\tilde{t}} + \frac{1}{2}\tilde{w}\tilde{w}\right) - \tilde{y} \tag{2}$$

where the dimensionless pressure is given by

$$\tilde{p} = \frac{kp}{\rho g}$$

and the frequency parameter is $S = gk/\omega^2$.

In SW the calculation of standing waves in deep water is considerably simplified by mapping the moving fluid region in the physical, or $\tilde{z} = \tilde{x} + i\tilde{y}$, plane into a fixed region in the $\zeta = \xi + i\eta$ plane. The image of the fluid region occupies the half-plane $\eta \leq o$. The required conformal map

$$\tilde{z} = \zeta + iZ(\zeta, \tilde{t}) \tag{3}$$

is determined as part of the solution. Z is an analytic function of its argument that, because of the symmetry and periodicity requirements, is given by the infinite series

$$Z(\zeta, \tilde{t}) = \sum_{p=o}^{\infty} a_p e^{-ip\zeta} \tag{4}$$

where the coefficients a_p are functions of time. Each a_p is calculated as a power series in ε, the (dimensionless) semi-amplitude of the wave at those instants of time when the water is at rest. The velocity potential is calculated as

$$\tilde{\phi} = \mathrm{Re}\ \{F[\zeta(\tilde{z}, \tilde{t}), \tilde{t}]\} \tag{5}$$

where $F = \Phi + i\Psi$, the complex potential in the transformed plane, has the representation

$$F(\zeta, \tilde{t}) = \sum_{p=o}^{\infty} c_p(\tilde{t}) e^{-ip\zeta} \tag{6}$$

Each c_p is also calculated as a power series in ε with coefficients that are Fourier polynomials in time. Both F and Z are $O(\varepsilon)$; thus for $\varepsilon = o$, (3) is merely an identity mapping.

The velocity field induced by periodic standing wave motion decays exponentially with depth. As was first shown by Miche (1944), the potential, on the other hand, contains an unattenuated component that is order ε^2. At great depths, therefore, this is the dominant contribu-

tion. From (2), the nonhydrostatic portion of the pressure as $\eta \to -\infty$ is given by

$$\lim_{\eta\to-\infty} \tilde{p} \equiv \tilde{p}_1 = -\frac{\Phi_{\tilde{t}}}{S} = -\frac{c_o'(\tilde{t})}{S} . \tag{7}$$

The solution presented in SW was calculated to $O(\varepsilon^{25})$ by delegating the coefficient arithmetic to a computer. The first few coefficients may be recognized as rational numbers from repetition in their decimal expansions. Through $O(\varepsilon^6)$, the series for $\tilde{p}_1$ is

$$\begin{aligned} \tilde{p}_1 = &-\frac{\varepsilon^2}{2}\cos 2\tilde{t} + \frac{\varepsilon^4}{8}(3\cos 2\tilde{t} + \cos 4\tilde{t}) \\ &- \frac{\varepsilon^6}{4}\left(\frac{46177}{39424}\cos 2\tilde{t} + \cos 4\tilde{t} + \frac{27}{512}\cos 6\tilde{t}\right) + O(\varepsilon^8) \end{aligned} \tag{8}$$

where the expansion for $S(\varepsilon)$ given in SW has also been used. Notice that $\tilde{p}_1(t)$ varies with twice the frequency of the surface displacement. Longuet-Higgins (1950), who computed the first term in (8), presents a simple physical explanation for the frequency doubling. For finite depth, however large, the center of gravity of the fluid region is displaced as the surface undulates. By symmetry the centroid moves through two complete cycles during each period of the surface wave. The pressure on the bottom, which supplies the necessary motive force, must therefore fluctuate in a similar manner with twice the frequency of the waves.

In Figure 1 we show the time variation of pressure at infinite depth for a fairly steep wave. In the figure $\varepsilon = 0.6$, about 10 per

cent short of the limiting wave that in SW is estimated to have a steepness of about 0.66. The pressure was computed as a Padé approximant formed from 12 terms in the series in (8). Padé approximants are rational fractions formed from a finite number of terms in a given power series. The results in the figure are drawn from the [6/6] approximant which has six terms in both the numerator and denominator. In general, the sequence of approximants formed from increasing numbers of terms in the series expansion of a function will converge much faster than the sequence of partial sums and will usually converge to the analytic continuation of the function when the argument lies outside of the radius of convergence. A somewhat more complete description of the procedure is given in SW ; general theory of Padé approximants may be found in Baker (1975). The convergence of the sequence of approximants to the series (8) suggests that the data in the figure are accurate to at least one part in 10^3. Note that $\tilde{p}$ is an even function of ωt with period π . In Figure 2 we display the corresponding undulations of the free surface for this values of ε as ωt varies between 0 and $\pi/2$. For $\frac{\pi}{2} \leq \omega t \leq \pi$, the profiles are left-right reflections of those shown.

In general $\tilde{p}_1$ achieves its maximum value at $\omega t = \pi/2$ and its minimum at $t = 0$. Figure 3 shows the magnitude of the pressure variation, $\tilde{p}_1(\pi/2) - \tilde{p}_1(o)$, plotted versus ε^2 for amplitudes ranging from infinitesimal up to the limiting wave. The pressure difference dips slightly as the limiting value of ε^2 is approached. We note that similar behavior was observed in the variation of the parameter S presented in SW .

In both Figures 1 and 3, the leading-order result, computed from the first term in (8), is shown for comparison. For very steep waves the simple theory overestimates the pressure by as much as 40 per cent. This is in stark contrast to the frequency calculation, for example, where the linear theory result, $\omega = \sqrt{gk}$, is never in error by more than 5 per cent.

Another application of the results presented in SW is the computation of the pressure on a breakwater due to wave action. Two-dimensional periodic standing waves will result from the normal incidence of a periodic progressive wave train upon a vertical barrier. We will be concerned here only with those instants of time when there is a crest or a trough at the breakwater. Thus, at $t = 0$, the surface achieves its maximum displacement and the fluid is instantaneously at rest. The Bernoulli equation assumes the simplified form

$$\tilde{p} = -\frac{\Phi_{\tilde{t}}}{S} - \eta - \mathrm{Re}\{Z\} . \tag{9}$$

The image of the free surface is $\eta = 0$; there $\tilde{p}$ is zero. Substituting expansions (4) and (6) in (9) and evaluating on $\eta = 0$, we obtain immediately

$$c_p'(\tilde{t}) + S\, a_p = 0$$

for $p = 0, 1, 2, \ldots$. Hence $F_{\tilde{t}} + SZ = 0$ and the pressure is given simply by

$$\tilde{p} = -\eta .$$

At these instants of time, therefore, the contours of constant η are the isobars in the physical plane.

In order to plot pressure versus depth, it is necessary to calculate the vertical displacement corresponding to a given value of η. We take the imaginary part of (3) with $\xi = 0$ and $\xi = \pi$ to compute the ordinates beneath a crest and a trough respectively and obtain

$$y(\xi = 0) = \eta + \sum_{p=o}^{\infty} a_p e^{p\eta}$$

and

$$y(\xi = \pi) = \eta + \sum_{p=o}^{\infty} a_p (-1)^p e^{p\eta} .$$

In SW it is shown that the coefficienta a_p have expansions of the form

$$a_p = \sum_{n=o}^{\infty} \alpha_{pn} \varepsilon^{p+2n}$$

where

$$\alpha_{pn} = \sum_{\ell=0}^{\left[\frac{2n+p}{2}\right]} \alpha_{pn\ell} \cos(p + 2n - 2\ell)\tilde{t} .$$

Here [ ] is the integer-part function. For $\tilde{t} = 0$, these equations become

$$y\begin{pmatrix} 0 \\ \pi \end{pmatrix} = \eta + \sum_{k=1}^{\infty} (\pm\varepsilon)^k h_k \tag{10a}$$

where

$$h_k = \sum_{\ell=0}^{[k/2]} e^{(k-2\ell)\eta} \sum_{m=o}^{[k/2]} \alpha_{k-2\ell,\ \ell,\ m} \quad . \tag{10b}$$

A table of coefficients $\alpha_{pn}(0)$ may be found in SW .

The series in (10a) involves both odd and even powers of ε ; from the 25th-order solution developed in SW , Padé approximants through [12/12] may be forned. We use these approximants to sum the series for $\varepsilon = 0.55$ and present the resulting pressure profiles in Figure 4. The sequence of approximants converged to at least one part in 10^4.

As the depth increases, the two profiles merge asymptotically. The asymptote is not the hydrostatic pressure variation for the reasons discussed in detail above. Penney and Price (1952) present a figure equivalent to Figure 4 for their parameter $A = 0.5$ corresponding to about the same value of wave height. Their profiles are drawn so as to be asymptotic to the hydrostatic pressure. They were, apparently, unaware of Miche's (1944) result and appear to have lost the second-order unattenuated pressure variation. In addition, the pressure distribution beneath the crest which they present differs appreciably from the one in Figure 4 near the still-water level; the difference being about 25% at $y = 0$.

To our knowledge, no experimental measurements of standing wave pressures have yet been made. In light of the significant applications of the theory in both geophysics and coastal engineering, it would seem

to be a most worthwhile exercise. Reasonably periodic standing waves have been produced in laboratory wave tanks by several investigators. The pressure variation on the walls and bottom of these tanks could be obtained with little additional difficulty.

References

Baker, G. A. Jr. 1975 Essentials of Padé Approximants, Academic Press, New York.

Longuet-Higgins, M. S. 1950 Phil. Trans. Roy. Soc. Lond. A, 243, 1.

Miche, M. 1944 Ann. Ponts Chauss. 2, 42.

Penney, W. G. & Price, A. T. 1952 Phil. Trans. Roy. Soc. Lond. A 244, 254.

Schwartz, L. W. & Whitney, A. K. 1980 J. Fluid Mech. (to appear)

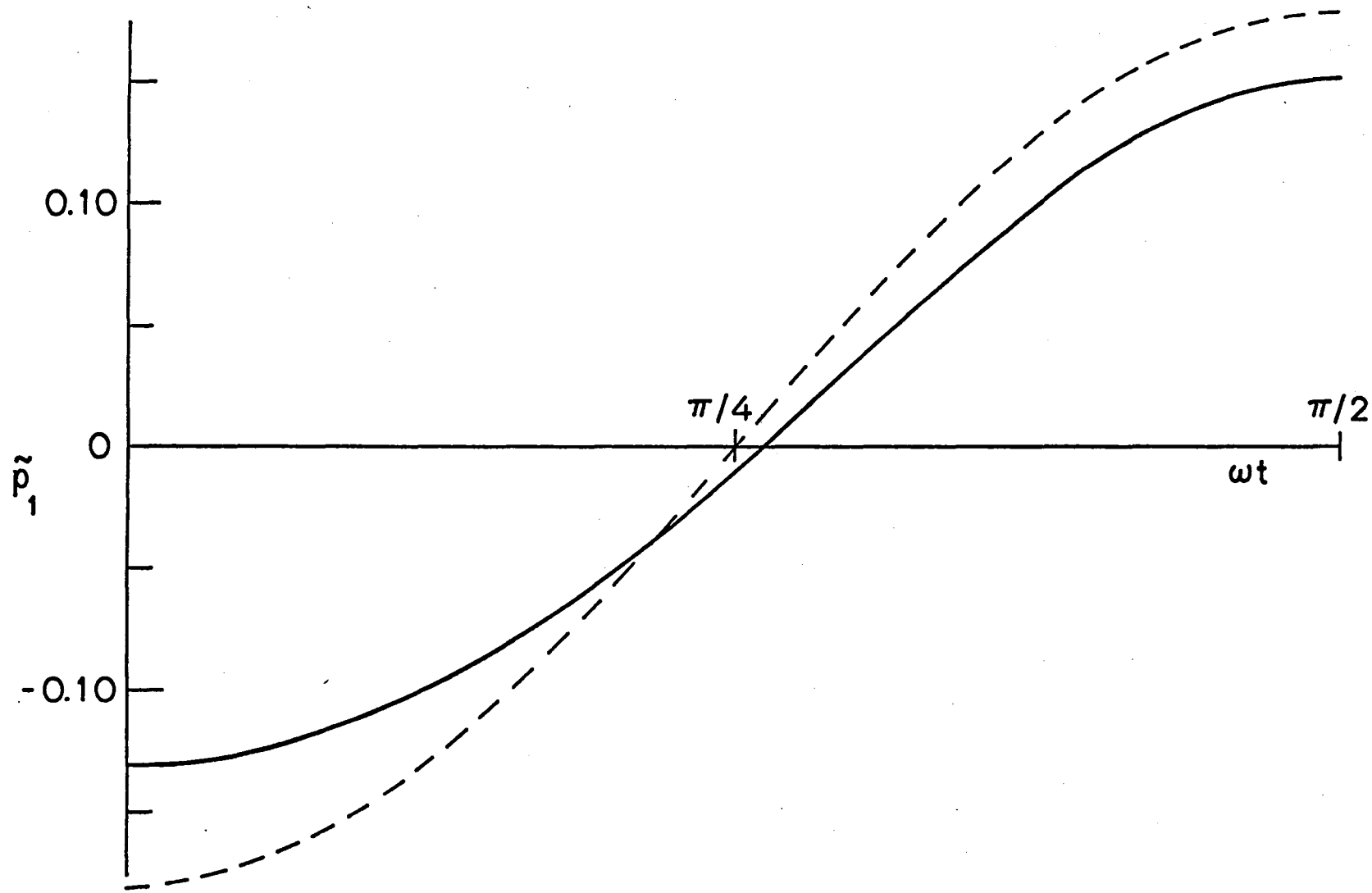

Figure 1. Time variation of pressure at infinite depth, $\varepsilon = 0.6$; - - - leading-order theory.

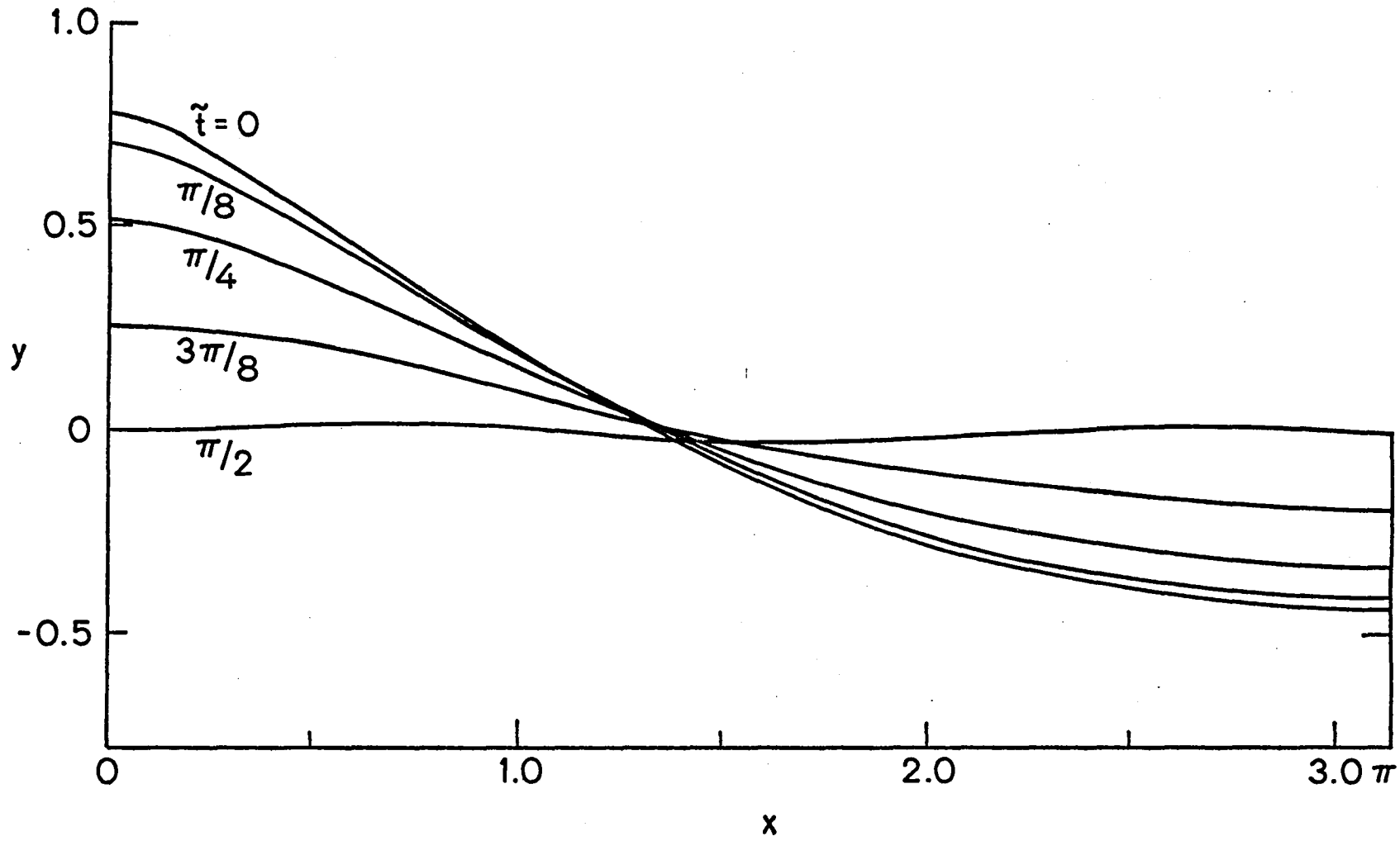

Figure 2. Surface profiles versus time, $\varepsilon = 0.6$.

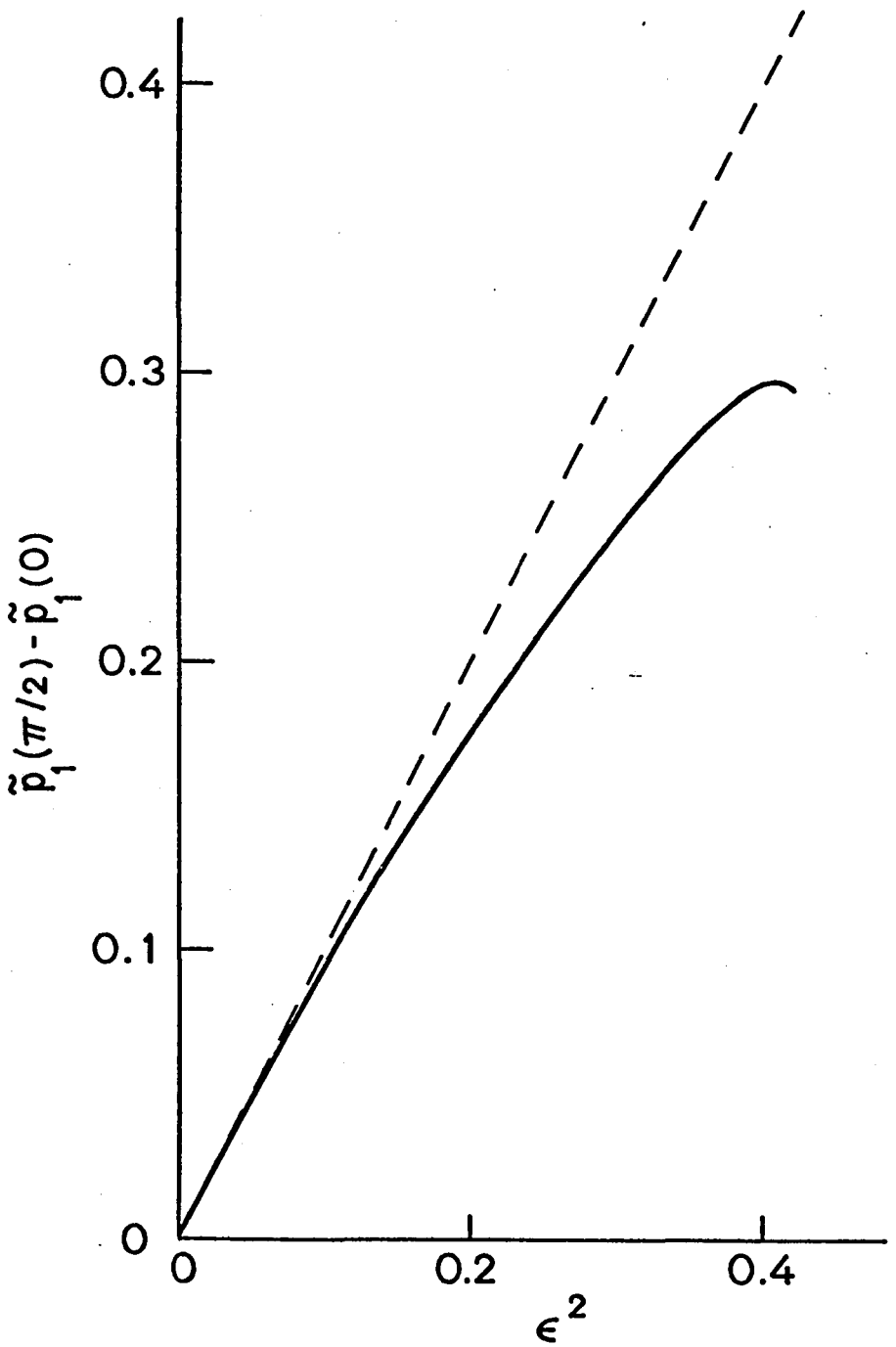

Figure 3. Magnitude of pressure variation at infinite depth;
- - - leading-order theory

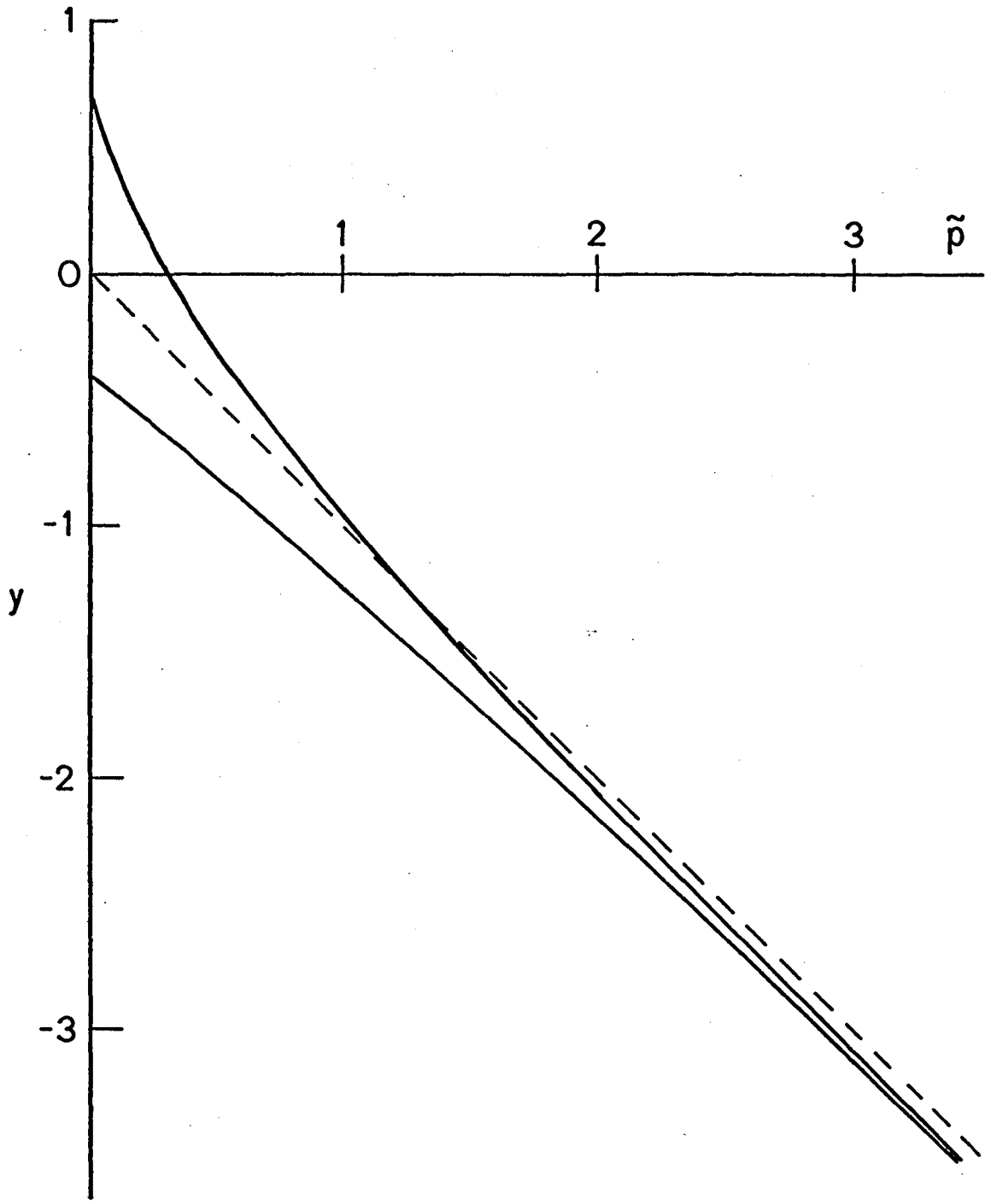

Figure 4. Pressure distribution vertically below a crest and a trough, $t = 0$, $\varepsilon = 0.55$.

End of Document